Redox Transformation of Arsenic by Fe(II)-Activated Goethite (α-FeOOH)

KATJA AMSTAETTER,[†,§] THOMAS BORCH,[‡] PHILIP LARESE-CASANOVA,[†] AND ANDREAS KAPPLER*[,†]

Geomicrobiology, Center for Applied Geosciences, University of Tuebingen, Germany, and Department of Soil and Crop Sciences and Department of Chemistry, Colorado State University, Fort Collins, Colorado 80523-1170

Received April 29, 2009. Revised manuscript received August 29, 2009. Accepted September 11, 2009.

The redox state and speciation of the metalloid arsenic (As) determine its environmental fate and toxicity. Knowledge about biogeochemical processes influencing arsenic redox state is therefore necessary to understand and predict its environmental behavior. Here we quantified arsenic redox changes by pH-neutral goethite [α-Fe^{III}OOH] mineral suspensions amended with Fe(II) using wet-chemical and synchrotron X-ray absorption (XANES) analysis. Goethite itself did not oxidize As(III) and, in contrast to thermodynamic predictions, Fe(II)-goethite systems did not reduce As(V). However, we observed rapid oxidation of As(III) to As(V) in Fe(II)-goethite systems. Mössbauer spectroscopy showed initial formation of ^{57}Fe-goethite after ^{57}Fe(II) addition plus a so far unidentified additional Fe(II) phase. No other Fe(III) phase could be detected by Mössbauer, EXAFS, SEM, XRD, or HR-TEM. This suggests that reactive Fe(III) species form as an intermediate Fe(III) phase upon Fe(II) addition and electron transfer into bulk goethite but before crystallization of the newly formed Fe(III) as goethite. In summary this study indicates that in the simultaneous presence of Fe(III) oxyhydroxides and Fe(II), as commonly observed in environments inhabited by iron-reducing microorganisms, As(III) oxidation can occur. This potentially explains the presence of As(V) in reduced groundwater aquifers.

Introduction

Arsenic (As) is a health threat in many countries all over the world. About 150 million people worldwide are estimated to be exposed to elevated arsenic concentrations in drinking water (*1*). Anthropological and geological sources affect arsenic concentrations in soils, sediments, surface water, and groundwater (*2*). The mechanisms controlling retention and release of arsenic at the solid−water interface have been subject to extensive studies (*2, 3*). However, the relevant processes are often site-specific and controlled by the present aqueous geochemistry, hydrology, or anthropogenic impact (*4*). This has led to contrary findings in the literature about the mechanisms responsible for arsenic release/sorption and for arsenic redox reactions both in the environment but also in laboratory systems. It has been suggested for example that reductive dissolution of arsenic-bearing Fe(III) minerals in groundwater aquifers leads to a release of the adsorbed arsenic (*5, 6*). However, as recently shown, microbial iron(III) reduction can also lead to the formation of stable Fe(II)-containing mineral phases and thus to arsenic sorption and immobilization (*7*−*9*). Bacteria can also change arsenic mobility by As(V) reduction as well as by As(III) oxidation (*10, 11*). Reduction of As(V) to As(III) for example leads to enhanced mobility and toxicity of the reduced species (*10, 12, 13*).

The differences in mobility and toxicity of the two most environmentally relevant arsenic species, As(III) and As(V) oxyanions, make an in-depth understanding of arsenic redox chemistry important. Abiotic oxidation of dissolved As(III) has been detected in solutions containing oxygen and Fe(II) or oxygen and MnO_2 (*14*−*16*). Chemical oxidation of As(III) has also been observed on the solid phase of reactive iron barriers (*17*), in the presence of Fe(IV) formed by H_2O_2-dependent Fenton reactions (*18*), under alkaline conditions in the presence of Fe(0) or Fe(III) oxyhydroxides (*19*) and by lake sediments (*14*). Although thermodynamically unfavorable, As(V) was also found under anoxic conditions in natural groundwater samples (*5*).

To our knowledge, no detailed studies have been published on the redox interaction of arsenic with green rusts or systems containing Fe(III) mineral and aqueous/sorbed Fe(II) although such systems showed reduction of organic compounds (*20, 21*) as well as heavy metals (*22, 23*). Goethite interacting with dissolved Fe(II) showed the highest redox activity in comparison to the other Fe(III) (oxy)hydroxides (*24*).

Based on the knowledge gaps outlined above, the goal of this study was to quantify the redox transformation of As(V) and As(III) in systems containing goethite and aqueous Fe(II). Dissolved and sorbed arsenic species were quantified by wet-chemical analysis and synchrotron-based X-ray absorption techniques (XANES). The mineral phases were characterized by scanning electron microscopy (SEM), high-resolution transmission electron microscopy (HR-TEM), μ-X-ray diffraction (μ-XRD), Fe extended X-ray absorption fine structure (Fe-EXAFS), and by Mössbauer spectroscopy.

Experimental Section

Chemicals and Minerals. All chemicals used in this study were of analytical grade. Arsenic solutions were prepared from sodium salts ($NaAsO_2$, Na_2HAsO_4).

The Fe(II) stock solution was prepared by adding 3.63 g (0.065 mmol) metal iron (Fe(0)) to 100 mL anoxic 1 M HCl in a screw cap bottle with a rubber septum under anoxic conditions. The suspension was heated to 80 °C while gently stirring. After 2 h no more hydrogen evolution was observed indicating that Fe(0) oxidation stopped. The suspension was filtered in an anoxic glovebox (0.2 μm PTFE filter) to remove any residual metal iron. The concentration of Fe(II) was determined colorimetrically by the ferrozine assay (see below). An isotopically pure ^{57}Fe(II) solution was prepared similarly from ^{57}Fe(0) (96% pure, ChemGas) according to Williams and Scherer (*25*).

Goethite (Bayferrox 920 Z) was provided by LANXESS Deutschland GmbH (for detailed characterization see Supporting Information (SI)). Isotopically pure ^{56}Fe-goethite was synthesized using isotopically pure ^{56}Fe(0) (99.9% pure, ChemGas) according to Williams and Scherer (*25*). The mineral purity and absence of significant amounts of contaminations were verified by SEM, XRD, and in case of minerals with natural abundance of Fe-isotopes, also by TOC

* Corresponding author phone: +49-7071-2974992; fax: +49-7071-5059; e-mail: andreas.kappler@uni-tuebingen.de.
† University of Tuebingen.
‡ Colorado State University.
§ Current address: Department of Environmental Engineering, Norwegian Geotechnical Institute, 0806 Oslo, Norway.

10.1021/es901274s

Published on Web 10/07/2009

(total organic carbon), XRF (X-ray fluorescence), and Mössbauer analysis (see also SI). The mineral specific surface area was determined by N_2−BET measurements (Bayferrox goethite: 9.2 m^2/g, ^{56}Fe-goethite: 44 m^2/g).

Fe(II)-Goethite Arsenic Redox Transformation Experiments. Suspensions with a goethite concentration of 50 m^2/L (5.4 g/L) were prepared anoxically in screw cap bottles with a Teflon coated rubber septum. The mineral powder was suspended in DI water, homogenized for 24 h in an overhead shaker, and washed twice with DI water. The stirred suspension was purged with N_2 for 1 h and transferred into an anoxic chamber (Braun, Germany; 100% N_2). Dissolved Fe(II) (0.7 M stock solution, prepared as described above) and anoxic 0.2 M NaOH were added alternating with equilibration periods of several hours between the additions until an Fe(II) concentration in solution of 1 mM and a pH of 7 was reached (total amount of Fe(II) added was about 2 mM). Saturation for $Fe(OH)_2$ is not reached under these conditions (see SI). After 17 h of incubation, aliquots of 25 mL suspension were distributed for duplicate batches into 50 mL serum bottles. As(III) or As(V) were added to a final concentration of 1.2 mg/L, and the bottles were shaken in the dark (to prevent photochemical reactions) at room temperature. After sampling at 0, 6, and 7 days, the content of one bottle was filtered through a syringe filter (0.45 μm, nitrocellulose acetate, Millipore). The homogenously distributed thin paste of reacted goethite (including adsorbed/transformed Fe(II) or arsenic) on the filter was dried (~2 min), then sealed between two pieces of Kapton polyimide film to prevent oxidation while minimizing X-ray absorption, and packed in anoxic vials individually until measurement at the Stanford Synchrotron Radiation Lightsource (SSRL). Subsamples for SEM and XRD analysis were collected as well as liquid samples for Fe(II) and arsenic identification and quantification. The Fe(II)-goethite arsenic redox transformation experiments were repeated once giving comparable results with regard to As(III) oxidation. The results shown in this study originate from one of these two experiments. Within each experiment, all batch mixtures were prepared in duplicate.

^{57}Fe(II)-^{56}Fe-Goethite Experiment. Isotopically pure, water-rinsed and dried ^{56}Fe-goethite was suspended in anoxic DI water in the glovebox. The ^{56}Fe-goethite concentration was 50 m^2/L (1.14 g/L). ^{57}Fe(II) concentration and pH were adjusted as described in the section above and were set to 1 mM and pH 7, respectively (total amount of Fe(II) added was about 1.1 mM). The suspension was incubated for 23 h, filtered (see above) and the filter was mounted between Kapton tape for Mössbauer measurements.

Analytical Methods. Separation of the aqueous arsenic species was done using an anion exchange cartridge according to (*26*). This cartridge retains As(V) but not As(III) within the pH range of 4−9 with a removal efficiency of 98% for As(V) and a recovery of As(III) of 95% (*26*). After separation, aqueous arsenic was quantified by ICP-MS (Elan 600, PE SCIEX, Perkin-Elmer). Detection limit for arsenic was 1 μg/L. Samples were stabilized in 0.1 M HNO_3 (4.5 mL sample + 0.5 mL 1 M HNO_3) and stored in the fridge until measurement. Rhodium was added as internal standard to each sample to a final concentration of 1 ppm Rh.

Dissolved iron was quantified using the ferrozine assay (*27*). In order to measure total iron (Fe(tot)) concentrations, aliquots were reduced with 10% w/v $NH_2OH \times HCl$ dissolved in 1 M HCl. Fe(II) and Fe(tot) samples were mixed with a 0.1% w/v solution of ferrozine in 50% w/v ammonium acetate buffer. Absorbance was measured at 562 nm in microtiter plates with a plate reader (FlashScan 550 microplate reader, Analytik Jena AG, Germany).

The specific surface area of iron minerals was determined by the BET method with a Gemini 2375 surface area analyzer with N_2 as adsorbing gas. Mineral samples were degassed and dried for 30 min under vacuum at 105 °C, before measuring a five-point-BET-curve.

Mössbauer spectra were collected with a constant acceleration drive system in transmission mode and with a ^{57}Co source at room temperature. Samples were mounted in a close-cycle exchange-gas cryostat (Janis, U.S.) that allowed cooling of the sample to 4.2 K. Spectra were calibrated against a spectrum of alpha-Fe metal foil collected at room temperature. Spectra calibration and fitting was performed with Recoil software (University of Ottawa, Canada) using Voigt based spectral lines (for details see SI).

For micro-X-ray diffraction (μ-XRD), samples were grinded in an agate mortar, prepared on a Si single crystal silicon wafer, and covered with a polyethylene foil to prevent oxidation. The μ-XRD-device (Bruker D8 Discover XRD instrument, Bruker, Germany) with a Co K_α X-ray tube (30 kV, 30 mA) allows measurements at a spot diameter of 50 or 300 μm (28). The EVA 10.0.1.0 software was used to merge the three measured overlapping frames of 30° 2θ (GADDS area detector). The mineral phases were identified using the PDF-database licensed by the International Centre for Diffraction Data (ICDD).

Extended X-ray absorption fine structure (EXAFS) and X-ray absorption near-edge structure (XANES) spectroscopy was performed at the Stanford Synchrotron Radiation Lightsource (SSRL) on beamlines 10−2 and 11−2, respectively. The storage ring was operated at 3.0 GeV and at currents between 60 and 100 mA. The Fe-EXAFS analytical procedures used here were similar to those described previously; for details see SI and refs *29 and 30*. A Si(220) monochromator was utilized for energy selection at the arsenic K-edge and sample fluorescence was measured with a Ge detector. The samples were maintained at 5 K during the data collection to prevent sample beam damage (i.e., beam induced redox reactions) using an Oxford Instruments CF1208 continuous flow liquid helium cryostat (see SI). Arsenic K-edge spectra were internally calibrated with sodium arsenate (11,874 eV). Linear combination fitting (LCF) of the sample spectra was performed using the arsenic model compounds. Precision of fitting arsenic species from XANES spectra is estimated to be 5% (*31*). For details about As analysis see SI.

Mineral samples for scanning electron microscopy (SEM) were prepared under anoxic conditions on an Al-stub covered with a conductive graphite tape. The sample was coated with a 45 nm Au coating (SCD 005/CEA 035 sputter, BAL-TEC). Images were obtained with an electron microscope (SEM LEO-1450 VP, LEO electron microscopy) with an acceleration voltage of 15−20 kV at a working distance of 5−12 mm (from six samples we analyzed at least two spots each at different magnifications).

For high resolution transmission electron microscopy (HR-TEM) aliquots of a goethite and a Fe(II)-goethite suspension were taken. After centrifugation the solids were washed twice with anoxic water and dried. Minerals were resuspended in methanol and placed on a holey carbon grid. HR-TEM images were taken at a JEOL 2100-F electron microscope (*32*) from two samples. Based on a preview of seven spots at a regular TEM, two images per sample were taken at the HR-TEM.

Results

Arsenic Redox Changes in Fe(II)-Goethite Systems. Arsenic redox changes were followed and quantified both in solution and at the mineral surface after incubation of As(III) or As(V) with goethite and Fe(II)-goethite. X-ray absorption near edge spectroscopy (XANES) was used for speciation and quantification of mineral surface-associated arsenic. Both XANES analysis (Figure 1, Table 1) and quantification of arsenic in solution (Table 1) showed neither As(III) oxidation nor As(V) reduction by pure goethite. When adding Fe(II) to goethite

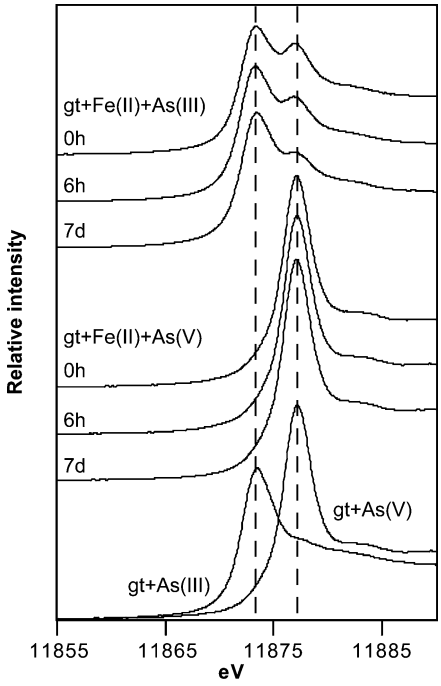

FIGURE 1. As-XANES spectra showing arsenic redox transformation by reactive iron species at time point zero (directly after mixing), after 6 h and after 7 days. The experiments contained goethite (gt) and Fe(II) with either As(III) or As(V). For comparison As(V) and As(III) adsorbed to goethite without Fe(II) are shown at the bottom.

suspensions we did not observe As(V) reduction even after 7 days of incubation indicating that the Fe(II)-goethite system was unable to reduce As(V) to As(III) under these conditions (Figure 1, Table 1). However, when adding As(III) to a Fe(II)-goethite suspension we observed rapid oxidation of As(III), both in solution and in the solid phase (Figure 1, Table 1). XANES analysis showed 21, 16, and 12% As(V) (formed by oxidation of As(III)) at the mineral surface directly after mixing (0 h), after 6 h and after 7 days, respectively. The total amount of arsenic in solution decreased from 377 to 128 μg/L after 7 days of reaction (Table 1), indicating increasing adsorption over time. pH values dropped less than 0.5 units at sampling time points after incubation with arsenic (data not shown).

Mineral Formation and Transformation in Fe(II)-Goethite Systems. To understand the arsenic redox changes observed in our experiments it is necessary to identify the reactive iron species responsible for the As(III) oxidation. We therefore performed Mössbauer spectroscopy, Fe-EXAFS, XRD, SEM, and HR-TEM analysis in an attempt to elucidate the structure of the minerals present. In order to identify potentially reactive iron phases formed upon addition of Fe(II), we used the advantage of Mössbauer spectroscopy to specifically detect the ^{57}Fe isotope. We prepared a goethite/Fe(II) suspension using ^{56}Fe-goethite and aqueous ^{57}Fe(II) (without addition of arsenic). The transformation of the added ^{57}Fe(II) at the goethite surface was then selectively detected by Mössbauer spectroscopy without the background signal of the underlying ^{56}Fe-goethite. Fitting of the obtained spectrum (measured at 77K, fitting parameters are given in the SI) resulted in a sextet (95%) indicating the presence of ^{57}Fe-goethite that is formed by oxidation of the sorbed ^{57}Fe(II) by the underlying goethite (*25, 32, 33*) (Figure 2). In addition to the goethite sextet, we observed a doublet (5%), indicating the presence of a ^{57}Fe(II) species, which could possibly represent Fe(II) hydroxide, green rust or adsorbed Fe(II). However, the presence of Fe(II) hydroxide could be ruled out first because the saturation for $Fe(OH)_2$ is not reached in our systems (see SI) and second because the quadrupole splitting distribution value is too low (2.60 ± 0.05 mm/s here compared to 3.0 mm/s for pure Fe(II) hydroxide) (*34*). The presence of a detectable Fe(II) phase in similar goethite-Fe(II) systems has not been reported previously (*25*), (*33*), (*35*). In contrast to these studies where the goethite mineral surface was not saturated with Fe(II), we had seven times more Fe(II) removed than surface sites available (see SI) indicating a significant oversaturation of the surface with Fe(II) compared to the other studies that did not show a detectable Fe(II) phase. This oversaturation combined with the different nature of the goethite used in our study, such as particle volume or semiconducting ability, were likely responsible for the formation of a detectable Fe(II) phase in our experiments.

HR-TEM images of pure goethite compared to Fe(II)-treated goethite rods showed no distinct changes in crystal structure (Figure 2). Similar structures were observed in a previous TEM study (*32*) where the authors also saw no differences between pure goethite and Fe(II)-treated goethite although they speculated that differences might be seen by HR-TEM. In our experiments XRD, Fe-EXAFS, and SEM analysis of the Fe(II)-goethite mixture after 7 days of incubation with and without added As(III) showed reflections (XRD), spectra (Fe-EXAFS) and structures (SEM) typical for goethite (Figure 2). No secondary iron minerals were observed or identified by SEM, XRD, and Fe-EXAFS. However, the amount of the Fe(II) phase (5% of the added dissolved ^{57}Fe(II)) detected by Mössbauer spectroscopy is very low and most likely not detectable by the other analytical methods used (due to the Fe EXAFS and XRD detection limits of approximately 5 mol % Fe and 5 wt %, respectively).

Discussion

Arsenic Redox Transformation by Fe(II)-Activated Goethite. Quantification of dissolved arsenic species separated by an ion exchange cartridge followed by ICP-MS analysis and of mineral-bound arsenic by synchrotron based X-ray absorption spectroscopy (XAS) allowed analysis and quantification of the arsenic redox speciation in our arsenic-goethite systems. Based on thermodynamic considerations for arsenic redox transformations in our Fe(II)-goethite system (SI Figure S2), reduction of As(V) to As(III) is expected to occur at neutral pH (Figure 3a, reaction 2a). Similar experiments with reactive Fe(II)-bearing mineral systems demonstrated reduction of heavy metals (Cr(IV), U(VI)) by carbonate green rust, Fe(II)-hematite systems. and iron-containing sediment particles (*22, 23*). In contrast to reduction of the dissolved chromate and uranyl which leads to formation of less toxic and immobile oxides and hydroxides, reduction of As(V) would enhance the risk potential of this metalloid due to the higher mobility and toxicity of As(III) (*2*). However, in our experiments we did not observe As(V) reduction by abiotic Fe(II)-goethite systems but rather As(III) oxidation in both the solid and the liquid phase (Figure 1; Table 1). Several mechanisms for As(III) oxidation are possible (Figure 3a). Since we observed no redox transformation in experiments with goethite in the absence of Fe(II), we can rule out the direct oxidation of As(III) by goethite in our systems (Figure 3a, reaction 2b), as it was suggested by Sun and Doner to occur in particular at lower pH values (pH 5) (*16*). Thermodynamic calculations for As(III) oxidation by goethite (and iron minerals such as ferrihydrite, magnetite, green rust and aqueous $Fe(OH)_3$) showed that oxidation of As(III) by these Fe(III) phases under our experimental conditions is energetically unfavorable (granted that all literature values used for the Gibb's free energy of formation have basically no error associated with them) although the redox potentials of As(III)/As(V) and Fe(II)/goethite redox couples are close to each other (see SI). Direct oxidation of As(III) by O_2 can also be excluded in our experiments due to strict anoxic experi-

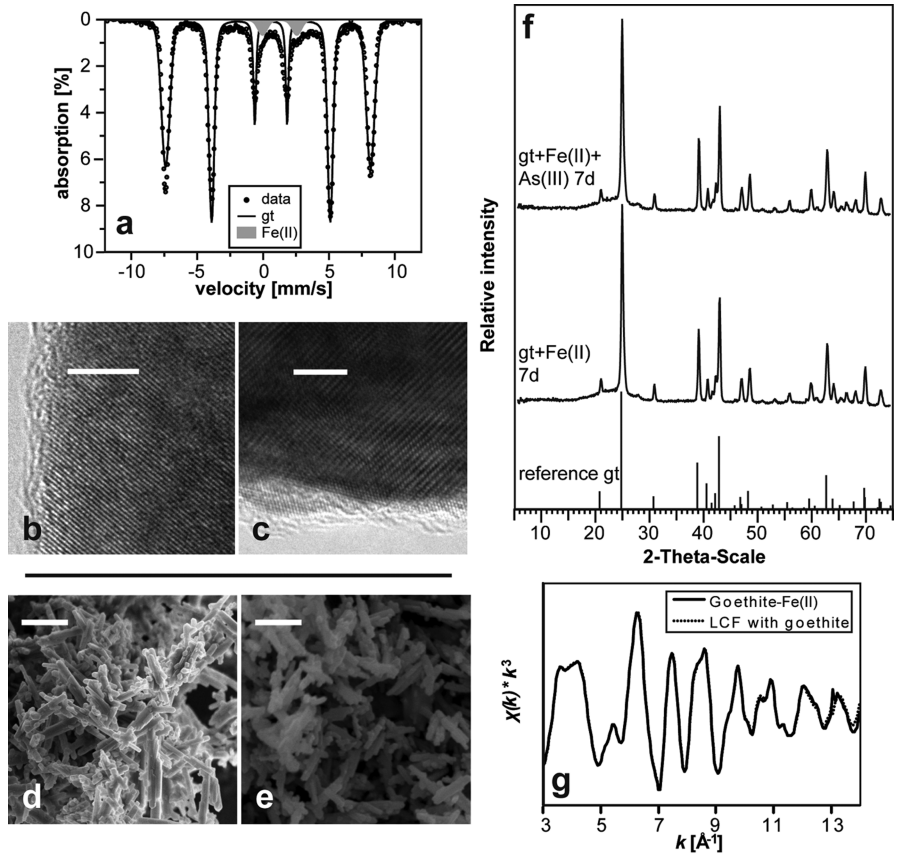

FIGURE 2. (a) Mössbauer spectrum of ^{56}goethite with adsorbed ^{57}Fe(II) measured at 77K showing a Fe(III) goethite sextet and a Fe(II) doublet. (b, c) High-resolution transmission electron microscopy (HR-TEM) images of (b) goethite and (c) Fe(II)-goethite systems after 4 days of incubation (size bar 5 nm). (d, e) SEM images of (d) goethite or (e) Fe(II)-goethite systems after 7 days of incubation (size bar 1 μm). (f) XRD patterns of Fe(II)-goethite and Fe(II)-goethite + As(III) after 7 days of incubation, showing reflections only for goethite. (g) k^3-weighted Fe-EXAFS spectrum of goethite reacted with Fe(II) and As(III) for 7 days (solid line) and linear combination fit (LCF; dotted line) using pure goethite with adsorbed As(III).

TABLE 1. Redox Speciation of Arsenic Sorbed to the Solid Phase and Arsenic in Solution for Abiotic Experiments with Goethite (gt) Amended with As(III)/As(V) or Goethite Amended with Fe(II) and As(III)/As(V)

		Solid phase[a]				Concentration in solution[b]				
		As(III) (%)	As(V) (%)	As(III) (ppm)	As(V) (ppm)	As(III) (%)	As(V) (%)	As(III) (μg/L)	As(V) (μg/L)	As in solution/ As tot
gt+Fe(II)+As(III)	0 h	79	21	119	32	86	14	324	53	0.31
	6 h	84	16	154	29	94	6	187	12	0.17
	7d	88	12	173	24	89	11	114	14	0.11
gt+Fe(II)+As(V)	0 h	[c]	100	[c]	221	[c]	[c]	[c]	[c]	0
	6 h	[c]	100	[c]	221	[c]	[c]	[c]	[c]	0
	7 d	[c]	100	[c]	221	[c]	[c]	[c]	[c]	0
Gt+As(III)	7 d	100	[c]	208	[c]	100	[c]	69	[c]	0.06
Gt+As(V)	7 d	[c]	100	[c]	221	[c]	[c]	[c]	[c]	0

[a] Determined by X-ray absorption near edge spectroscopy (XANES) [b] Determined by ICP-MS [c] Concentration below detection limit (1 μg/L).

mental conditions (Figure 3a, reaction 2c). The oxidation of As(III) by O_2 is a relatively slow process (*14*), even trace amounts of O_2 can therefore not explain the fast oxidation of As(III) observed in samples obtained right after As(III) addition to the Fe(II)-goethite mineral suspension. Additionally, the absence of O_2 in our experiments excludes the previously described As(III) oxidation in presence of O_2 and Fe(II) (*15, 18, 36*). The potential for a Fenton's reaction induced oxidation of As(III) by reactive hydroxyl radicals was also considered since aqueous systems exposed to ultraviolet and visible light can cause the formation of hydrogen peroxide (i.e., H_2O_2) (*37*). However, Fenton's reaction does not seem to be a plausible explanation for the oxidation of As(III) since the reaction had only been described in presence of O_2 leading to H_2O_2 formation (e.g., photochemically) or after addition of H_2O_2 (*18, 36, 37*). Both scenarios do not apply for our system since all experiments were done under strictly anoxic conditions and can therefore not explain the observed oxidation. Emett and Khoe (*38*) described As(III) oxidation in the dark in presence of chloride and absence of oxygen,

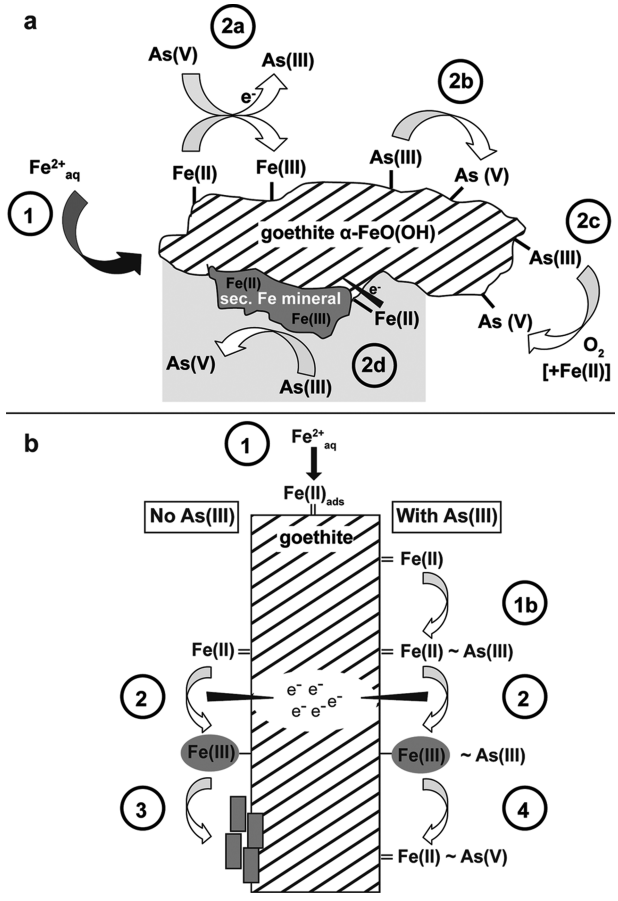

FIGURE 3. (a) Scheme summarizing possible redox reactions in a system containing dissolved Fe(II), goethite and the arsenic species As(III) or As(V). (1) Adsorption of dissolved Fe(II), (2a) reduction of As(V) by adsorbed Fe(II), (2b) direct oxidation of As(III) at the goethite surface, (2c) oxidation of As(III) by O_2, and (2d) As(III) oxidation by secondary mixed-valent iron mineral phases (the latter one probably being relevant for our study and therefore highlighted in gray). (b) Suggested mechanism of formation of a reactive Fe(III) intermediate phase formed upon (*1*) adsorption of dissolved Fe(II), i.e., Fe^{2+}, (1b) binding of As(III) to the sorbed Fe(II) (*2*), electron transfer into the bulk goethite phase forming the reactive Fe(III) intermediate. This intermediate either (*3*) transforms/crystallizes into goethite or (*4*) oxidizes As(III) via the reactive Fe(III) intermediate.

i.e., conditions similar to the ones in our study. However, in their experiments As(III) oxidation took place at pH 1.5 with high concentrations of Fe(III) being in solution and not at neutral pH (with extremely low Fe(III) in solution) where we observed As(III) oxidation. Furthermore As(III) oxidation in their experiments was slowed down by dissolved Fe(II) which we added in surplus. We also tested the potential for synchrotron radiation induced oxidation of As(III) by comparing multiple rapid XANES scans performed on the same sample location but no beam-induced redox change was observed when analyzed at 5K (see SI Figure S1). In addition, As oxidation was also observed in synchrotron independent measurements where As(V) was quantified in the aqueous phase by ICP-MS (Table 1) thereby further eliminating the potential for synchrotron induced oxidation of As(III). We therefore conclude that the As(III) oxidation observed in our experiments was caused by a reactive Fe(III) species or secondary iron mineral phase that was formed during electron transfer from Fe(II) to goethite (Figure 3a, reaction 2d).

Identity of Reactive Iron Phases Formed in the Fe(II)-Goethite System. Fe-EXAFS, XRD, and SEM analysis did not indicate the presence of any crystalline or amorphous mineral phase other than goethite (Figure 2). There was also no evidence for the formation of a new iron phase based on HR-TEM imaging after 4 days of reaction of goethite with aqueous Fe(II) (Figure 2). However, Mössbauer spectroscopy analysis of a system containing isotopically pure ^{56}Fe-goethite and ^{57}Fe(II) allowed us to selectively trace the fate of the initially present dissolved ^{57}Fe(II). Upon addition of aqueous ^{57}Fe(II), we detected a so far unidentified ^{57}Fe(II)-containing compound, possibly green rust or a sorbed Fe(II)-species. Model calculations of Fe(II) sorption to goethite by Hiemstra and van Riemsdijk (*39*) suggested a combination of Fe(II) sorption and Fe(II) surface oxidation. This is in agreement with our experiments which led to the presence of adsorbed ^{57}Fe(II) and ^{57}Fe-goethite formation, respectively. According to their calculations, the predominance of one or the other mechanism depends mainly on pH variations just around pH 7. The lack of another Fe(III) signal in addition to the Fe(III)-goethite signal questions the presence of the mixed Fe(II)−Fe(III) phase green rust, but does not necessarily exclude it. The expected Fe(III) signal for green rust could be masked by the dominant goethite signal and the broad Fe(II) signal and may not be resolved in the spectrum due to its low content. Although green rusts formed in oxic and anoxic Fe(0)-containing systems have been shown to oxidize As(III) (*17, 40, 41*), a very recent lab study demonstrated that carbonate green rust neither caused reduction of As(V) nor oxidation of As(III) (*42*). Therefore the influence of green rust on the redox state of arsenic remains controversial and cannot be resolved in our system.

In addition to the ^{57}Fe(II)-signal, we also observed the formation of a ^{57}Fe(III)-mineral phase, namely goethite (although it cannot be excluded that other Fe(III) phases were present in amounts below the Mössbauer detection limit of approximately 2%). Similar to previous studies (*25, 33, 43*), this can be interpreted as a result of electron transfer from surface bound ^{57}Fe(II) to the underlying goethite and crystallization of the formed ^{57}Fe(III) as goethite. In a recent study, even complete atom exchange between the aqueous Fe(II) and goethite was described which indicated partial recrystallization of the goethite particles (*32*). The fact that goethite is formed from the added Fe(II) and no other Fe(III) mineral phases were detected suggests that the reactive Fe(III) phase that is responsible for As(III) oxidation in our experiments is formed as a reactive intermediate phase. This intermediate stage could be present during the electron transfer from sorbed Fe(II) to the bulk goethite and before the structural reorientation of this Fe(III) (the original Fe(II)) and its final crystallization as goethite (Figure 3b). This intermediate Fe(III) species could then interact with As(III), e.g., via ternary complex formation (see next section) leading to As(III) oxidation. Evidence for the presence of a short-lived but very reactive intermediate comes from the observation that the kinetics of As(III) oxidation in our system obviously is very fast. Specifically, we observed the highest extent of As(III) oxidation immediately after mixing of all components (Figure 1, Table 1). Previous isotope exchange studies lead to the conclusion that the atom exchange between dissolved and solid iron is an initially fast and then slower continuous process. Its extent depends on mineral size, Fe(II) concentration and incubation time (*32, 44*−*46*). Although As(III) should be oxidized by the reactive intermediate until either Fe(II) or As(III) is fully reacted, we observed that the reaction stopped as a specific As(V) to As(III) ratio was reached. This could be due to several reasons: (i) reaching equilibrium of the redox reaction (see discussion of the E_h-pH diagrams for As(III)/As(V) and Fe(II)/goethite in the SI), (ii) saturation of the bulk goethite with transferred

electrons from Fe(II) and As(III), or (iii) limitation of the iron atom exchange (limited number of reactive sites) due to arsenic sorption on the iron mineral surface. Jones et al. (*44*) for example showed a decrease in atom exchange of different iron minerals in presence of silicate or natural organic matter. A detailed quantification of the iron pool participating in atom exchange and changes in the exchange rate over time could potentially provide further insight into the As(III)-oxidizing process and how the arsenic−iron surface complexes affect the reactivity of the system.

Role of Ternary Goethite-Fe(II)−As(III) Complexes. Due to the strong sorption affinity of arsenic to iron, surface complexes between arsenic and the iron surface are expected. After mixing goethite with dissolved Fe(II), the present surface species that can interact with arsenic are structural Fe(III), sorbed Fe(II), and the potential intermediate Fe(III) species, respectively. Model calculations by Hiemstra and van Riemsdijk (*39*) and Dixit and Hering (*47*) showed that more As(III) is adsorbed by goethite in presence of increasing amounts of Fe(II). They suggested the formation of ternary binuclear-bidentate complexes either in the form of goethite-As(III)−Fe(II) (*39*) or goethite−Fe(II)−As(III) (*47*). Such complexes may even facilitate electron transfer inbetween the three reactants. Although both studies did not consider redox transformations of arsenic in their calculations, it would be conceivable that in our as well as in their experiments the presence of an inner-sphere complex of goethite−$Fe(II)_2$−As(III) could have led to a transfer of two electrons from the two Fe(II) atoms to goethite followed by the formation of a reactive intermediate goethite−$Fe(III)_2$−As(III) complex (Figure 3b). The intermediate Fe(III) phase (discussed above) with a potentially enhanced redox activity could now act as an oxidant for As(III) forming a goethite−$Fe(II)_2$−As(V) complex (Figure 3b). Since more As(III) sorption to goethite in the presence of Fe(II) was determined based on ICP analysis of the total soluble arsenic concentration in the supernatant by Dixit and Hering (*47*), it is likely that the increased As(III) sorption observed by these authors was due to As(III) oxidation (in the goethite−$Fe(III)_2$−As(III) complex) and thus As(V) adsorption rather than formation of ternary goethite−Fe(II)−As(III) complexes per se. It is widely recognized that As(V) and As(III) predominantly form inner-sphere complexes on iron (hydr)oxides, however, it is still not clear what structural arrangement predominates (*48*). The type of inner-sphere complex formed between As(V) and goethite (e.g., bidentate binuclear, bidentate mononuclear, or monodentate) will likely influence the sorption capacity of goethite. If the structural arrangement of As(V) adsorption is different than for As(III) then oxidation of As(III) could explain the observed increased As(III) adsorption in the presence of Fe(II).

Environmental Implications. Several studies have already described the occurrence of thermodynamically unstable As(V) under reducing conditions in natural environments (*49, 50*). This indicates that reductive dissolution of iron minerals or microbial arsenic reduction (*6, 51*) in anoxic zones may not be the only explanation for natural arsenic contamination and speciation. Oxidation of As(III) by a Fe(II)−goethite mixture may be an important mechanism that could be responsible for As(V) formation in anoxic aquifers similar to the recently reported As(III) oxidation by reactive semiquinone radicals formed during reduction of humic model compounds (*52*). Such processes could be specifically important in undisturbed aquifers as described by Polizotto et al. (*4*). Freshly deposited surface sediments were identified as main source for arsenic through iron and arsenic reduction under anoxic conditions. Released arsenic and Fe(II) was found to be transported then into deeper layers and into the groundwater (*4*). In deeper layers easy reducible iron phases (ferrihydrite) are most likely depleted after microbial reduction, but more crystalline minerals (goethite) would still be present. In situ formed Fe(II)−goethite could promote arsenic oxidation as described in this study. In general, hydraulic flow and thereby transport of dissolved reactants (Fe(II) or As(III)) seem to become more and more important for interpretation of field data (*4, 53*).

Acknowledgments

This work was funded by the German Research Foundation (DFG) and the German Ministry for Science and Education (BMBF project "Microactiv") to A.K. This work was supported in part by a National Science Foundation (NSF) CAREER Award (EAR 0847683) to T.B. We thank Dr. Christoph Berthold for help with XRD, Dr. Jörn Breuer and Bärbel Horn (University of Hohenheim) for ICP-MS measurements, and Robert Handler, Jonas Baltrusaitis, and Michelle Scherer (University of Iowa) for HR-TEM imaging and discussion. Portions of this research were carried out at the Stanford Synchrotron Radiation Lightsource, a national user facility operated by Stanford University on behalf of the U.S. Department of Energy, Office of Basic Energy Sciences. We thank Mike Massey, Jens Blotevogel, and Lyndsay Troyer (Colorado State University) for their invaluable help on this project.

Supporting Information Available

Detailed characterization of the used Fe minerals, additional Mössbauer and XAS data, and thermodynamic calculations for the As−Fe-system. Additionally, Figure S1 illustrates that beam-induced As(III) oxidation did not take place in our systems. Figure S2 shows thermodynamic calculations of arsenic and iron redox couples. This material is available free of charge via the Internet at http://pubs.acs.org.

Literature Cited

(1) Nriagu, J. O. , Arsenic poisoning through the ages. In *Environmental Chemistry of Arsenic*; Frankenberger, W. T. J., Ed.; Marcel Dekker, Inc.: New York, 2002; pp 1−26.
(2) Smedley, P. L.; Kinniburgh, D. G. A review of the source, behaviour and distribution of arsenic in natural waters. *Appl. Geochem.* **2002**, *17* (5), 517–568.
(3) Polizzotto, M. L.; Harvey, C. F.; Li, G.; Badruzzman, B.; Ali, A.; Newville, M.; Sutton, S.; Fendorf, S. Solid-phases and desorption processes of arsenic within Bangladesh sediments. *Chem. Geol.* **2006**, *228* (1−3), 97–111.
(4) Polizzotto, M. L.; Kocar, B. D.; Benner, S. G.; Sampson, M.; Fendorf, S. Near-surface wetland sediments as a source of arsenic release to ground water in Asia. *Nature* **2008**, *454* (7203), 505–508.
(5) Postma, D.; Larsen, F.; Minh Hue, N. T.; Duc, M. T.; Viet, P. H.; Nhan, P. Q.; Jessen, S. Arsenic in groundwater of the Red River floodplain, Vietnam: Controlling geochemical processes and reactive transport modeling. *Geochim. Cosmochim. Acta* **2007**, *71* (21), 5054–5071.
(6) Berg, M.; Stengel, C.; Trang, P. T. K.; Hung Viet, P.; Sampson, M. L.; Leng, M.; Samreth, S.; Fredericks, D. Magnitude of arsenic pollution in the Mekong and Red River Deltas−Cambodia and Vietnam. *Sci. Total Environ.* **2007**, *372* (2−3), 413–425.
(7) Kocar, B. D.; Herbel, M. J.; Tufano, K. J.; Fendorf, S. Contrasting effects of dissimilatory iron(III) and arsenic(V) reduction on arsenic retention and transport. *Environ. Sci. Technol.* **2006**, *40* (21), 6715–6721.
(8) Tufano, K. J.; Fendorf, S. Confounding impacts of iron reduction on arsenic retention. *Environ. Sci. Technol.* **2008**, *42* (13), 4777–4783.
(9) Islam, F. S.; Gault, A. G.; Boothman, C.; Polya, D. A.; Charnock, J. M.; Chatterjee, D.; Lloyd, J. R. Role of metal-reducing bacteria in arsenic release from Bengal delta sediments. *Nature* **2004**, *430* (6995), 68–71.
(10) Oremland, R. S.; Stolz, J. F. Arsenic, microbes and contaminated aquifers. *Trends Microbiol.* **2005**, *13* (2), 45–49.
(11) Kulp, T. R.; Hoeft, S. E.; Asao, M.; Madigan, M. T.; Hollibaugh, J. T.; Fisher, J. C.; Stolz, J. F.; Culbertson, C. W.; Miller, L. G.; Oremland, R. S. Arsenic(III) fuels anoxygenic photosynthesis in hot spring biofilms from Mono Lake, California. *Science* **2008**, *321* (5891), 967–970.

(12) Dixit, S.; Hering, J. G. Comparison of arsenic(V) and arsenic(III) sorption onto iron oxide minerals: implications for arsenic mobility. *Environ. Sci. Technol.* **2003**, *37* (18), 4182–4189.
(13) Masscheleyn, P. H.; Delaune, R. D.; Patrick, Jr., W. H. Effect of redox potential and pH on arsenic speciation and solubility in a contaminated Soil. *Environ. Sci. Technol.* **1991**, *25* (8), 1414–1419.
(14) Oscarson, D. W.; Huang, P. M.; Liaw, W. K. The oxidation of arsenite by aquatic sediments. *J. Environ. Qual.* **1980**, *9* (4), 700–703.
(15) Daus, B.; Mattusch, J.; Paschke, A.; Wennrich, R.; Weiss, H. Kinetics of the arsenite oxidation in seepage water from a tin mill tailings pond. *Talanta* **2000**, *51* (6), 1087–1095.
(16) Sun, X.; Doner, H. E. Adsorption and oxidation of arsenite on goethite. *Soil Sci.* **1998**, *163* (4), 278–287.
(17) Su, C.; Puls, R. W. Significance of Iron(II, III) Hydroxycarbonate green rust in arsenic remediation using zerovalent iron in laboratory column tests. *Environ. Sci. Technol.* **2004**, *38* (19), 5224–5231.
(18) Hug, S. J.; Leupin, O. Iron-catalyzed oxidation of arsenic(III) by oxygen and by hydrogen peroxide: pH-dependent formation of oxidants in the fenton reaction. *Environ. Sci. Technol.* **2003**, *37* (12), 2734–2742.
(19) Manning, B. A.; Hunt, M. L.; Amrhein, C.; Yarmoff, J. A. Arsenic(III) and arsenic(V) reactions with zerovalent iron corrosion products. *Environ. Sci. Technol.* **2002**, *36* (24), 5455–5461.
(20) Borch, T.; Inskeep, W. P.; Harwood, J. A.; Gerlach, R. Impact of ferrihydrite and anthraquinone-2,6-disulfonate on the reductive transformation of 2,4,6-trinitrotoluene by a gram-positive fermenting bacterium. *Environ. Sci. Technol.* **2005**, *39* (18), 7126–7133.
(21) Haderlein, S. B.; Pecher, K. , Pollutant reduction in heterogeneous Fe(II) / Fe(III) systems. In *Kinetics and Mechanisms of Reactions at the Mineral/ Water Interface*, Chapter 17; Sparks, D. L., Grundl, T., Eds.; American Chemical Society: Washington, DC, 1998; Vol. 715, pp 342−356.
(22) Liger, E.; Charlet, L.; Van Cappellen, P. Surface catalysis of uranium(VI) reduction by iron(II). *Geochim. Cosmochim. Acta* **1999**, *63* (19−20), 2939–2955.
(23) Williams, A. G. B.; Scherer, M. M. Kinetics of Cr(VI) reduction by carbonate green rust. *Environ. Sci. Technol.* **2001**, *35* (17), 3488–3494.
(24) Elsner, M.; Schwarzenbach, R. P.; Haderlein, S. B. Reactivity of Fe(II)-bearing minerals toward reductive transformation of organic contaminants. *Environ. Sci. Technol.* **2004**, *38* (3), 799–807.
(25) Williams, A. G. B.; Scherer, M. M. Spectroscopic evidence for Fe(II)-Fe(III) electron transfer at the iron oxide-water interface. *Environ. Sci. Technol.* **2004**, *38* (18), 4782–4790.
(26) Meng, X.; Korfiatis, G. P.; Christodoulatos, C.; Bang, S. Treatment of arsenic in Bangladesh well water using a household co-precipitation and filtration system. *Water Res.* **2001**, *35* (12), 2805–2810.
(27) Stookey, L. L. Ferrozine - A new spectrophotometric reagent for iron. *Anal. Chem.* **1970**, *42* (7), 779–781.
(28) Berthold, C.; Bjeoumikhov, A. ; Brügemann, L. , Fast XRD^2 microdiffraction with focusing X-Ray microlenses. *Part. Part. Syst. Charact.* **2008**, submitted.
(29) Moberly, J.; Borch, T.; Sani, R.; Spycher, N.; Şengör, S.; Ginn, T.; Peyton, B. Heavy metal-mineral associations in Coeur d'Alene river sediments: A synchrotron-based analysis. *Water, Air, Soil Pollut.* **2009**, *201* (1), 195–208.
(30) Borch, T.; Masue, Y.; Kukkadapu, R. K.; Fendorf, S. Phosphate imposed limitations on biological reduction and alteration of ferrihydrite. *Environ. Sci. Technol.* **2007**, *41* (1), 166–172.
(31) Bostick, B. C.; Chen, C.; Fendorf, S.; Arsenite retention mechanisms within Estuarine sediments of Pescadero, CA. *Environ. Sci. Technol.* **2004**, *38* (12), 3299–3304.
(32) Handler, R. M.; Beard, B. L.; Johnson, C. M.; Scherer, M. M. Atom exchange between aqueous Fe(II) and goethite: An Fe isotope tracer study. *Environ. Sci. Technol.* **2009**, *43* (4), 1102–1107.
(33) Cwiertny, D. M.; Handler, R. M.; Schaefer, M. V.; Grassian, V. H.; Scherer, M. M. Interpreting nanoscale size-effects in aggregated Fe-oxide suspensions: Reaction of Fe(II) with goethite. *Geochim. Cosmochim. Acta* **2008**, *72* (5), 1365–1380.
(34) Miyamoto, H. The magnetic properties of $Fe(OH)_2$. *Mater. Res. Bull.* **1976**, *11* (3), 329–335.
(35) Silvester, E.; Charlet, L.; Tournassat, C.; Gehin, A.; Greneche, J.-M.; Liger, E. Redox potential measurements and Mossbauer spectrometry of FeII adsorbed onto FeIII (oxyhydr)oxides. *Geochim. Cosmochim. Acta* **2005**, *69* (20), 4801–4815.
(36) Katsoyiannis, I. A.; Ruettimann, T.; Hug, S. J. pH dependence of fenton reagent generation and As(III) oxidation and removal by corrosion of zero valent iron in aerated water. *Environ. Sci. Technol.* **2008**, *42* (19), 7424–7430.
(37) Zuo, Y.; Hoigne, J. Evidence for photochemical formation of H_2O_2 and oxidation of SO_2 in authentic fog water. *Science* **1993**, *260* (5104), 71–73.
(38) Emett, M. T.; Khoe, G. H. Photochemical oxidation of arsenic by oxygen and iron in acidic solutions. *Water Res.* **2001**, *35* (3), 649–656.
(39) Hiemstra, T.; van Riemsdijk, W. H. Adsorption and surface oxidation of Fe(II) on metal (hydr)oxides. *Geochim. Cosmochim. Acta* **2007**, *71* (24), 5913–5933.
(40) Lien, H. L.; Wilkin, R. T. High-level arsenite removal from groundwater by zero-valent iron. *Chemosphere* **2005**, *59* (3), 377–386.
(41) Su, C. M.; Wilkin, R. T. , Arsenate and arsenite sorption on and arsenite oxidation by iron(II, III) hydroxycarbonate green rust. In *Advances in Arsenic Research*; Oxford University Press: New York, 2005; Vol. 915, pp 25−40.
(42) Jönsson, J.; Sherman, D. M. Sorption of As(III) and As(V) to siderite, green rust (fougerite) and magnetite: Implications for arsenic release in anoxic groundwaters. *Chem. Geol.* **2008**, *255* (1−2), 173–181.
(43) Larese-Casanova, P.; Scherer, M. M. Fe(II) Sorption on hematite: New insights Based on spectroscopic measurements. *Environ. Sci. Technol.* **2007**, *41* (2), 471–477.
(44) Jones, A. M.; Collins, R. N.; Rose, J.; Waite, T. D. The effect of silica and natural organic matter on the Fe(II)-catalysed transformation and reactivity of Fe(III) minerals. *Geochim. Cosmochim. Acta* **2009**, *73*, 4409–4422.
(45) Pedersen, H. D.; Postma, D.; Jakobsen, R.; Larsen, O. Fast transformation of iron oxyhydroxides by the catalytic action of aqueous Fe(II). *Geochim. Cosmochim. Acta* **2005**, *69* (16), 3967–3977.
(46) Mikutta, C.; Wiederhold, J. G.; Cirpka, O. A.; Hofstetter, T. B.; Bourdon, B.; Gunten, U. V. Iron isotope fractionation and atom exchange during sorption of ferrous iron to mineral surfaces. *Geochim. Cosmochim. Acta* **2009**, *73* (7), 1795–1812.
(47) Dixit, S.; Hering, J. G. Sorption of Fe(II) and As(III) on goethite in single- and dual-sorbate systems. *Chem. Geol.* **2006**, *228* (1−3), 6–15.
(48) Gustafsson, J. P.; Bhattacharya, P. Geochemical modelling of arsenic adsorption to oxide surfaces. In *Arsenic in Soil and Groundwater Environment. Trace Metals and Other Contaminants in the Environment*; Bhattacharya, P., Mukherjee, A.B., Bundschuh, J., Zevenhoven, R., Loeppert, R. H., Eds.; Elsevier: Maryland Heights, MO, 2007; Vol. 9, pp 159−206.
(49) de Mello, J.; Talbott, J.; Scott, J.; Roy, W.; Stucki, J. Arsenic speciation in arsenic-rich brazilian soils from gold mining sites under anaerobic incubation. *Environ. Sci. Pollut. Res.* **2007**, *14* (6), 388–396.
(50) Swartz, C. H.; Blute, N. K.; Badruzzman, B.; Ali, A.; Brabander, D.; Jay, J.; Besancon, J.; Islam, S.; Hemond, H. F.; Harvey, C. F. Mobility of arsenic in a Bangladesh aquifer: Inferences from geochemical profiles, leaching data, and mineralogical characterization. *Geochim. Cosmochim. Acta* **2004**, *68* (22), 4539–4557.
(51) Akai, J.; Izumi, K.; Fukuhara, H.; Masuda, H.; Nakano, S.; Yoshimura, T.; Ohfuji, H.; Md Anawar, H.; Akai, K. Mineralogical and geomicrobiological investigations on groundwater arsenic enrichment in Bangladesh. *Appl. Geochem.* **2004**, *19* (2), 215–230.
(52) Jiang, J.; Bauer, I.; Paul, A.; Kappler, A. Arsenic redox changes by microbially and chemically formed semiquinone radicals and hydroquinones in a humic substance model quinone. *Environ. Sci. Technol.* **2009**, *43*, 3639–3646.
(53) Kocar, B. D.; Polizzotto, M. L.; Benner, S. G.; Ying, S. C.; Ung, M.; Ouch, K.; Samreth, S.; Suy, B.; Phan, K.; Sampson, M.; Fendorf, S. Integrated biogeochemical and hydrologic processes driving arsenic release from shallow sediments to groundwaters of the Mekong delta. *Appl. Geochem.* **2008**, *23* (11), 3059–3071.

ES901274S